ASTRONOMY & ASTROPHYSICS
SUPPLEMENT SERIES

Astron. Astrophys. Suppl. Ser. **147**, 229–242 (2000)

Hα observations of Be stars

D.P.K. Banerjee, S.D. Rawat, and P. Janardhan[⋆]

Astronomy and Astrophysics Division, Physical Research Laboratory, Navrangpura, Ahmedabad 380 009, India

Received May 22; accepted September 11, 2000

Abstract. We present here the Hα spectra of 44 Be stars taken at a resolution of 0.5 Å. From the spectra, different emission line parameters have been deduced. A study of the correlations between different pairs of these parameters has been made with a view to understanding the mechanisms of line formation and shaping in Be stars.

Key words: Be stars — spectroscopy — line profiles

1. Introduction

Be stars are rapid rotating, early type stars characterised by Balmer line emission and IR excess. They exhibit irregular variability both, spectroscopically and photometrically. They are surrounded by a gaseous envelope, which is photoionized by the radiation from the central star. The subsequent recombination process gives rise to the hydrogen line emission. The emission line profiles of Be stars show a variety of shapes. One of the earliest models to explain these profiles was the rotational model by Struve (1931). Since then many emission line spectroscopic studies have been made to understand the Be phenomenon – particularly the process of envelope formation – and the physical parameters of the disk like its shape, size and kinematics.

Though great progress has been made in explaining the line profiles, by invoking general physical mechanisms, there are still certain aspects which are not well understood. Hummel & Dachs (1992) and Hummel (1994) have proposed an elegant mechanism which largely explains as to how symmetric profiles of the winebottle through the shell type, and their variations in between, can be generated by the same optically thick Keplerian envelope when viewed from different angles. One of the objectives of the present study is to see how observational data agree with the scenario put forward by Hummel (1994). Towards this end, we have acquired high resolution Hα profiles for a sample of 44 Be stars. Given the latitude of our observatory (24.653 °N), both, the northern and the mid-southern declination sources are accessible in the sky, and this is reflected in the choice of our sources.

The other objective behind this study was the idea of building up, or filling in the gaps in, the database of the emission line profiles of Be stars, particularly that for the temporal variability of the line profiles. The atlas by Hanuschik et al. (1996) shows that significant variations can occur in the profiles over protracted periods. Our data is intended to make an additional input for any comprehensive model, that may be constructed, for explaining the variability. Incidentally, concurrent with this study and with a view to getting a more complete picture, a near IR spectroscopic survey of about 30 Be stars was also made at a medium resolution ($R = 1000$). Some of the preliminary results on this may be found in Ashok & Banerjee (2000).

2. Observations

Observations of the 44 Be stars presented here, were carried out between April 1998 and January 2000 on the 1.2 m. Cassegrain telescope of the Mount Abu Infrared Observatory, India. All the observations were made using a fibre linked astronomical grating spectrograph (FLAGS), recently made operational (Banerjee et al. 1999). The spectrograph has a Czerny Turner configuration with $f/10$ optics of 1.5 m focal length. It is mounted on a bench and light from the $f/13$ Cassegrain focal plane of the telescope is fed into it by means of an optical fibre (fibre type FIP 320385415, manufactured by Polymicro Technologies, U.S.A.). The dispersing element is a 2400 lines/mm Jobin Yvon holographic grating used in first order. It gives a reciprocal dispersion of 0.135 Å pixel at the detector and a spectral coverage of about 25 Å per CCD frame. The resolving power of the spectrograph, constrained primarily by the 320 micron diameter of the core of

Send offprint requests to: D.P.K. Banerjee,
e-mail: orion@prl.ernet.in

⋆ Currently with: Department of Astronomy, University of Maryland, College Park, MD 20742, U.S.A

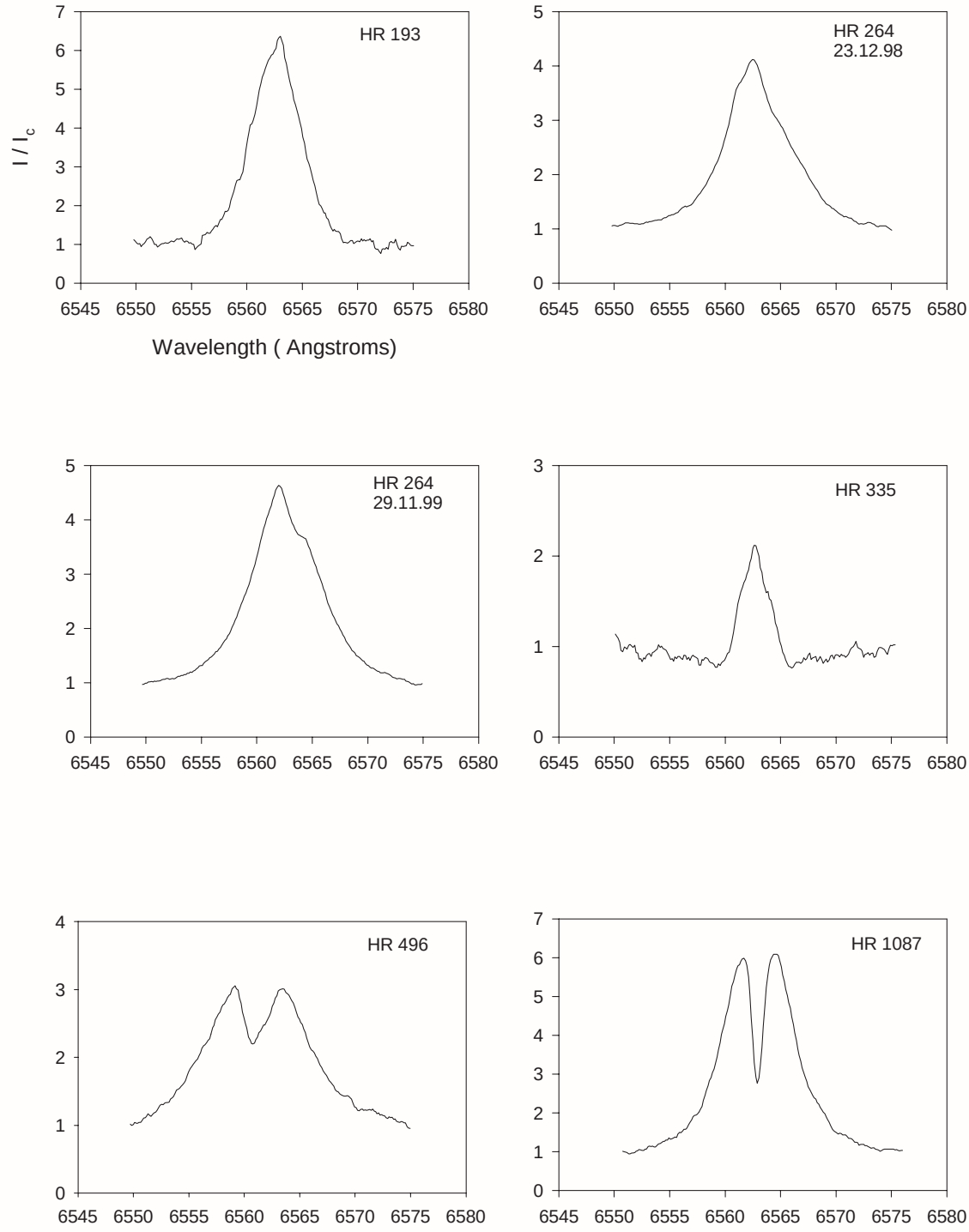

Fig. 1. Plots of the line profiles of different Be stars. The intensity plotted on the Y axis is relative and in units of the continuum level I_c

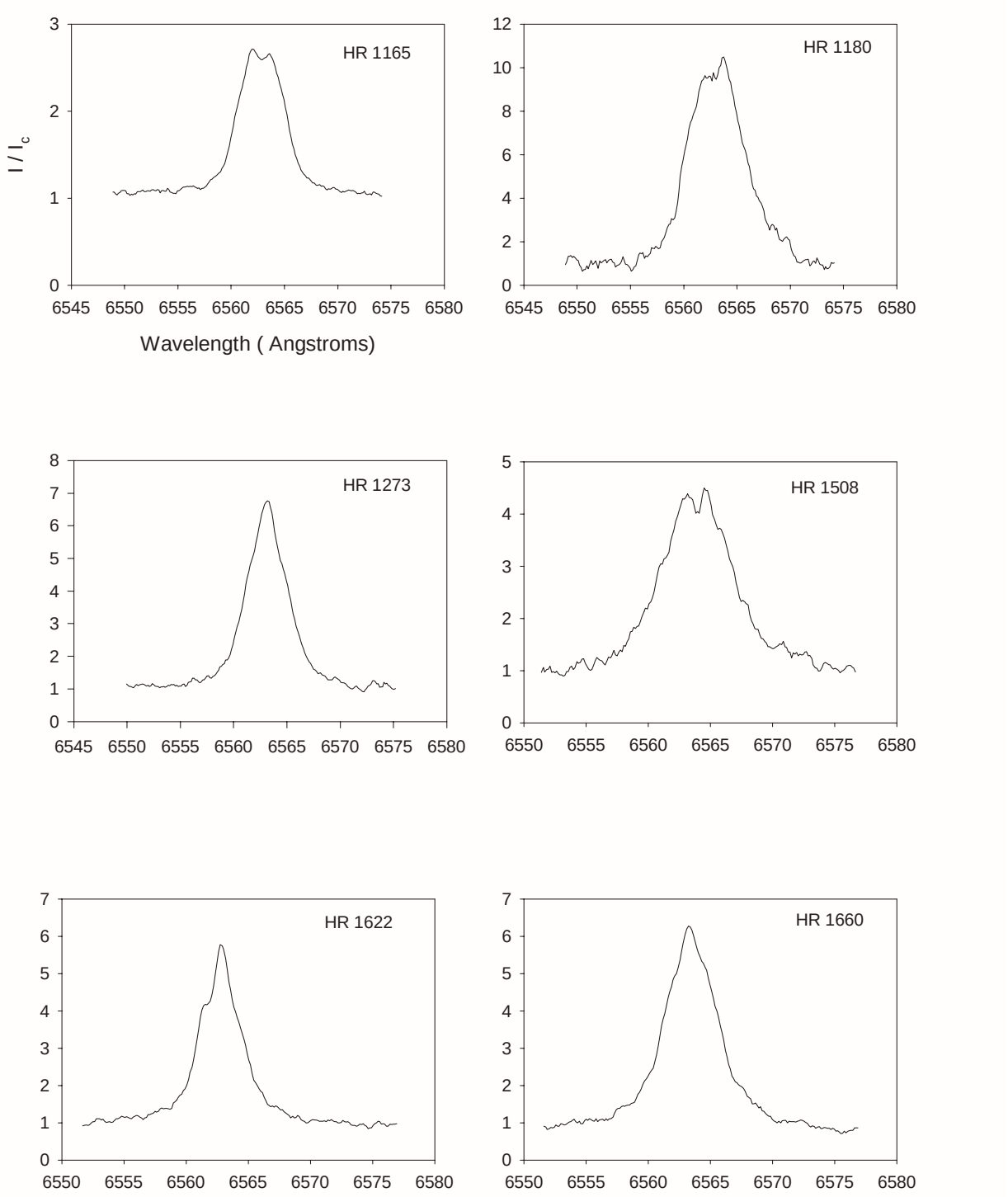

Fig. 2. Plots of the line profiles of different Be stars. The intensity plotted on the Y axis is relative and in units of the continuum level I_c

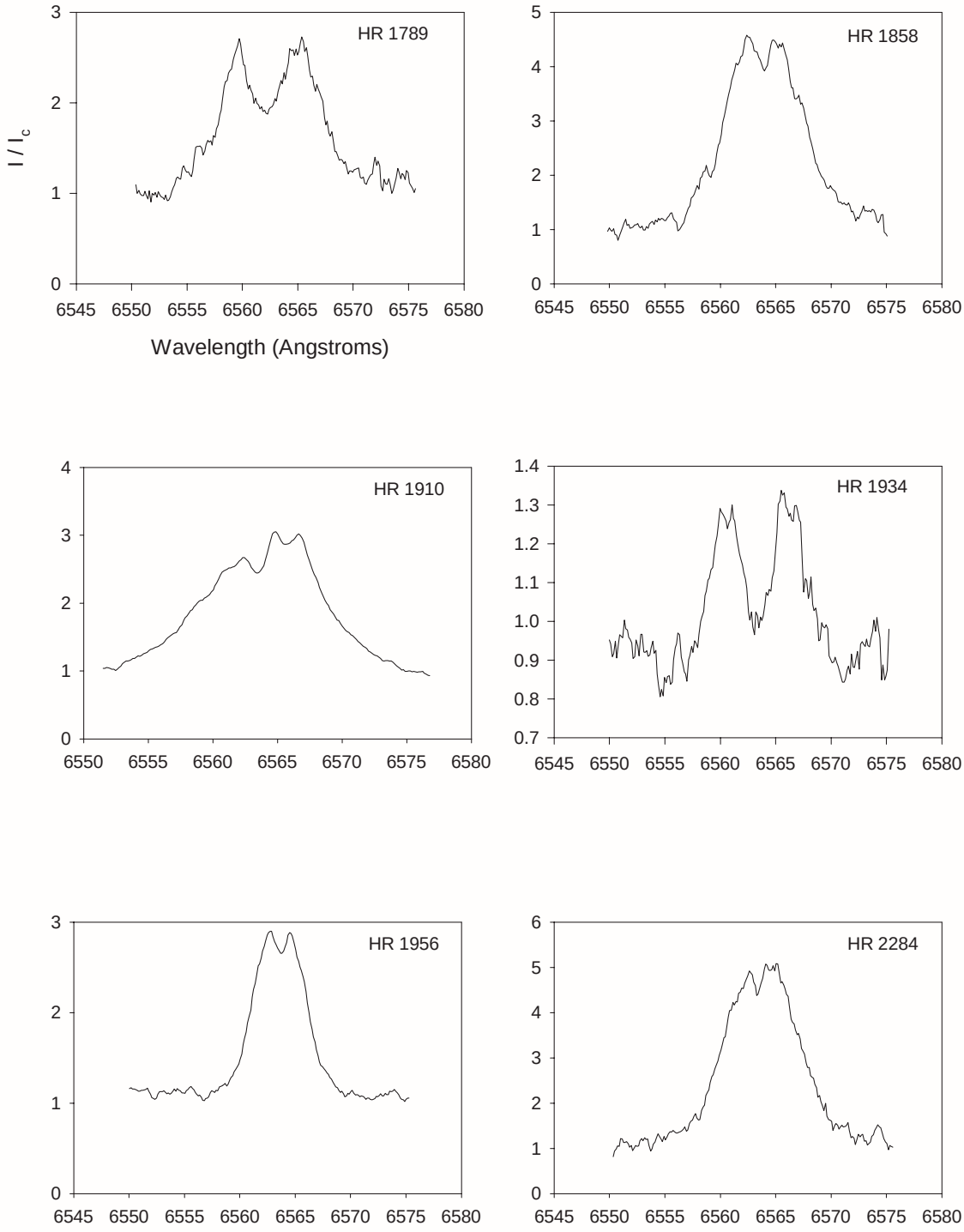

Fig. 3. Plots of the line profiles of different Be stars. The intensity plotted on the Y axis is relative and in units of the continuum level I_c

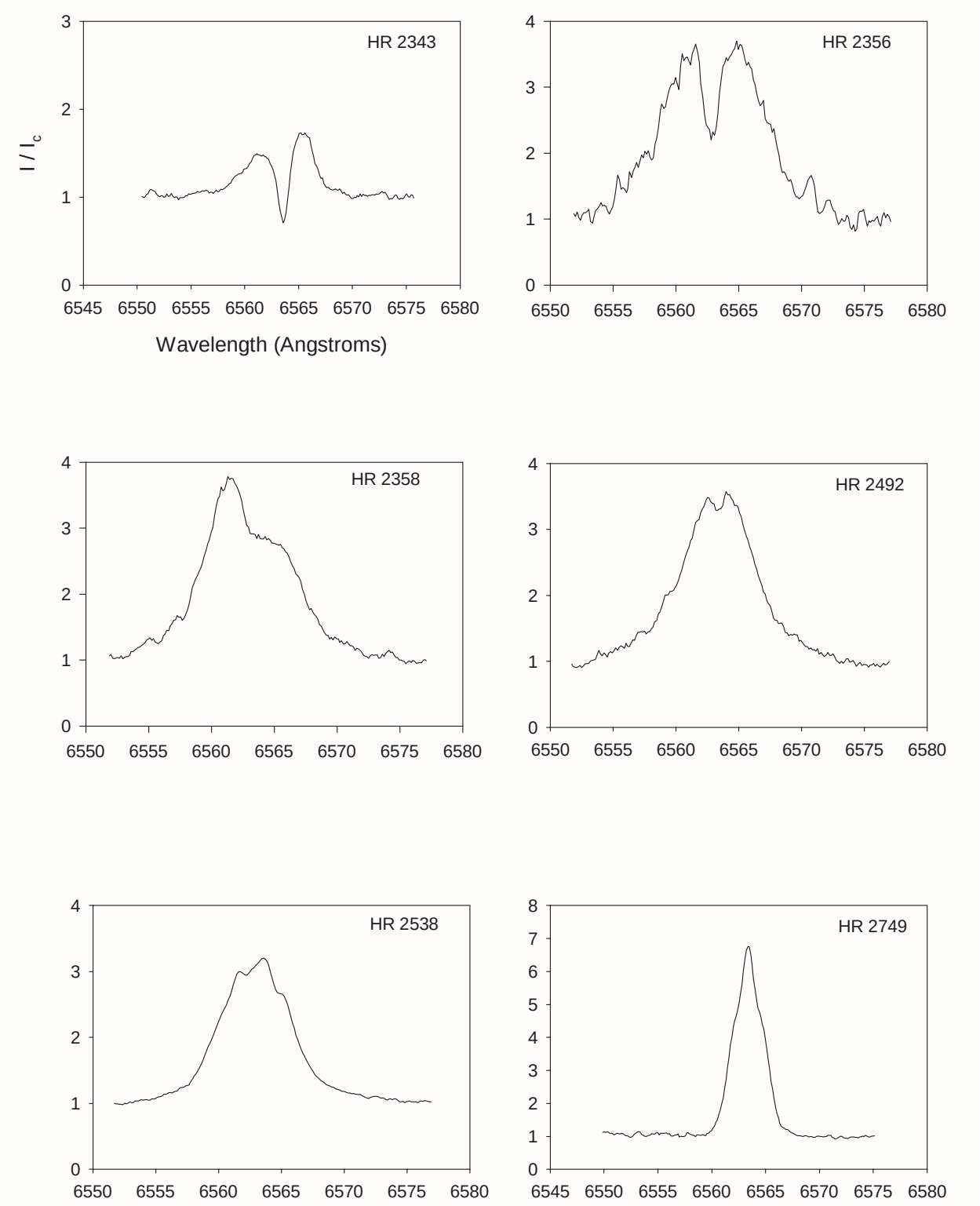

Fig. 4. Plots of the line profiles of different Be stars. The intensity plotted on the Y axis is relative and in units of the continuum level I_c

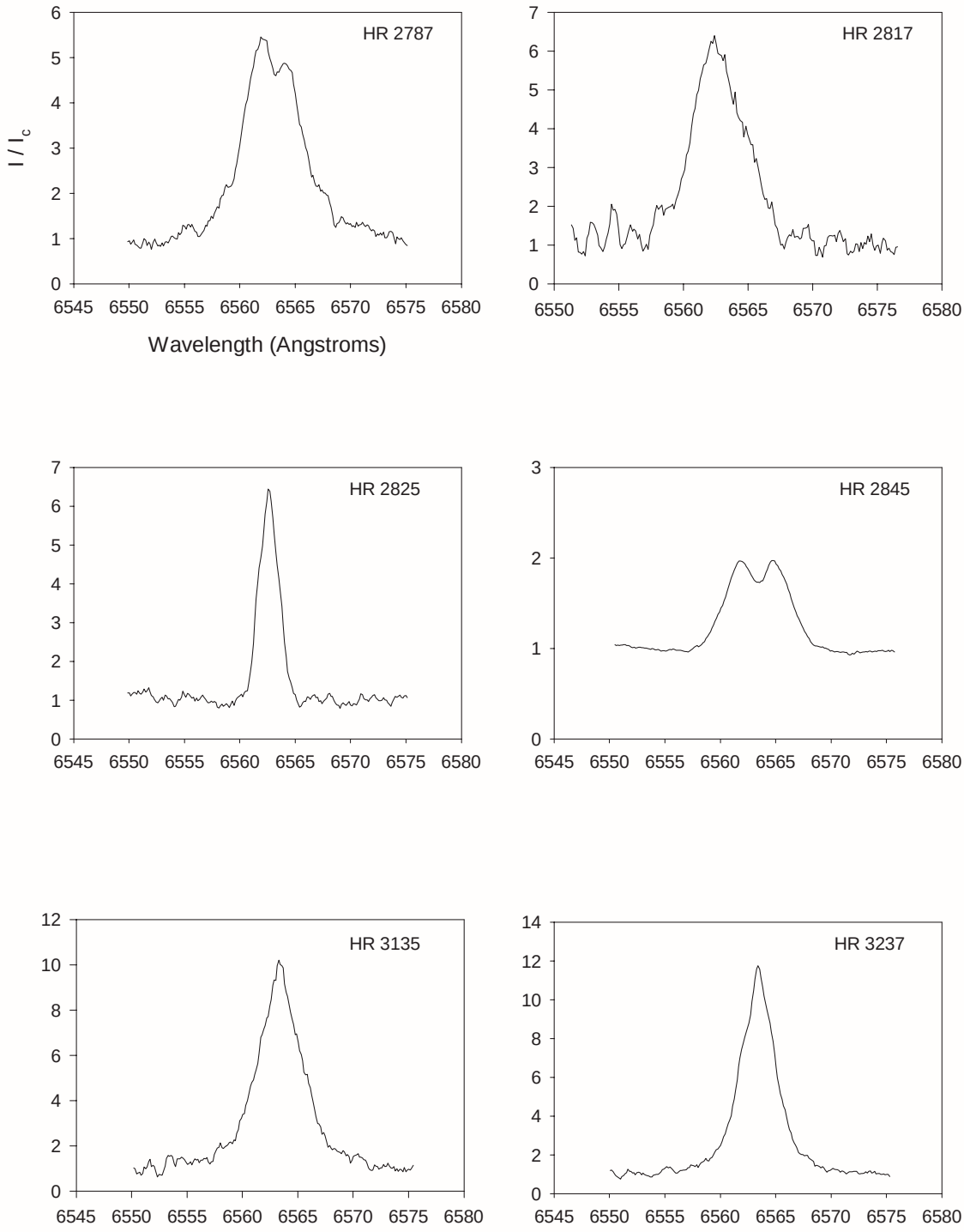

Fig. 5. Plots of the line profiles of different Be stars. The intensity plotted on the Y axis is relative and in units of the continuum level I_c

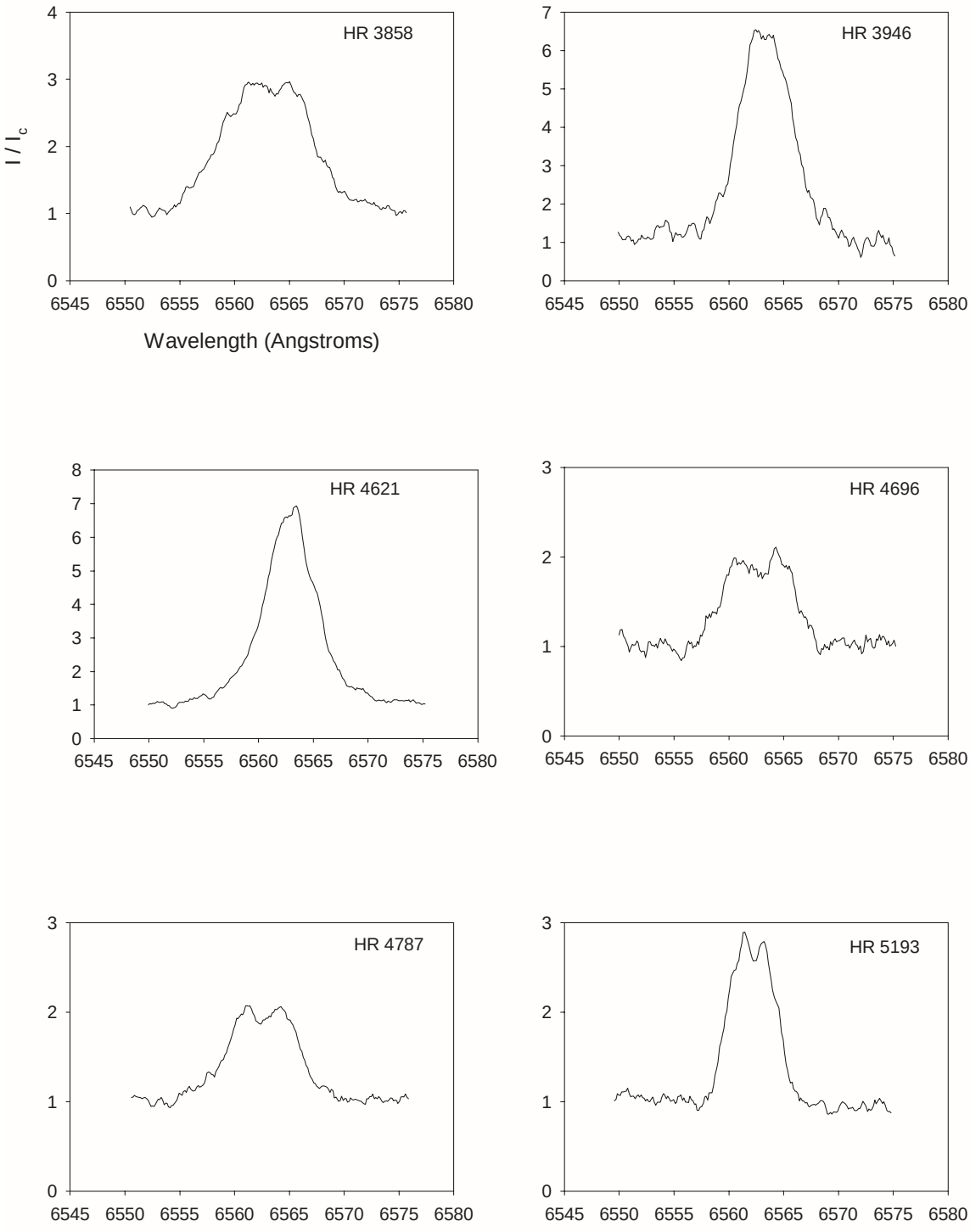

Fig. 6. Plots of the line profiles of different Be stars. The intensity plotted on the Y axis is relative and in units of the continuum level I_c

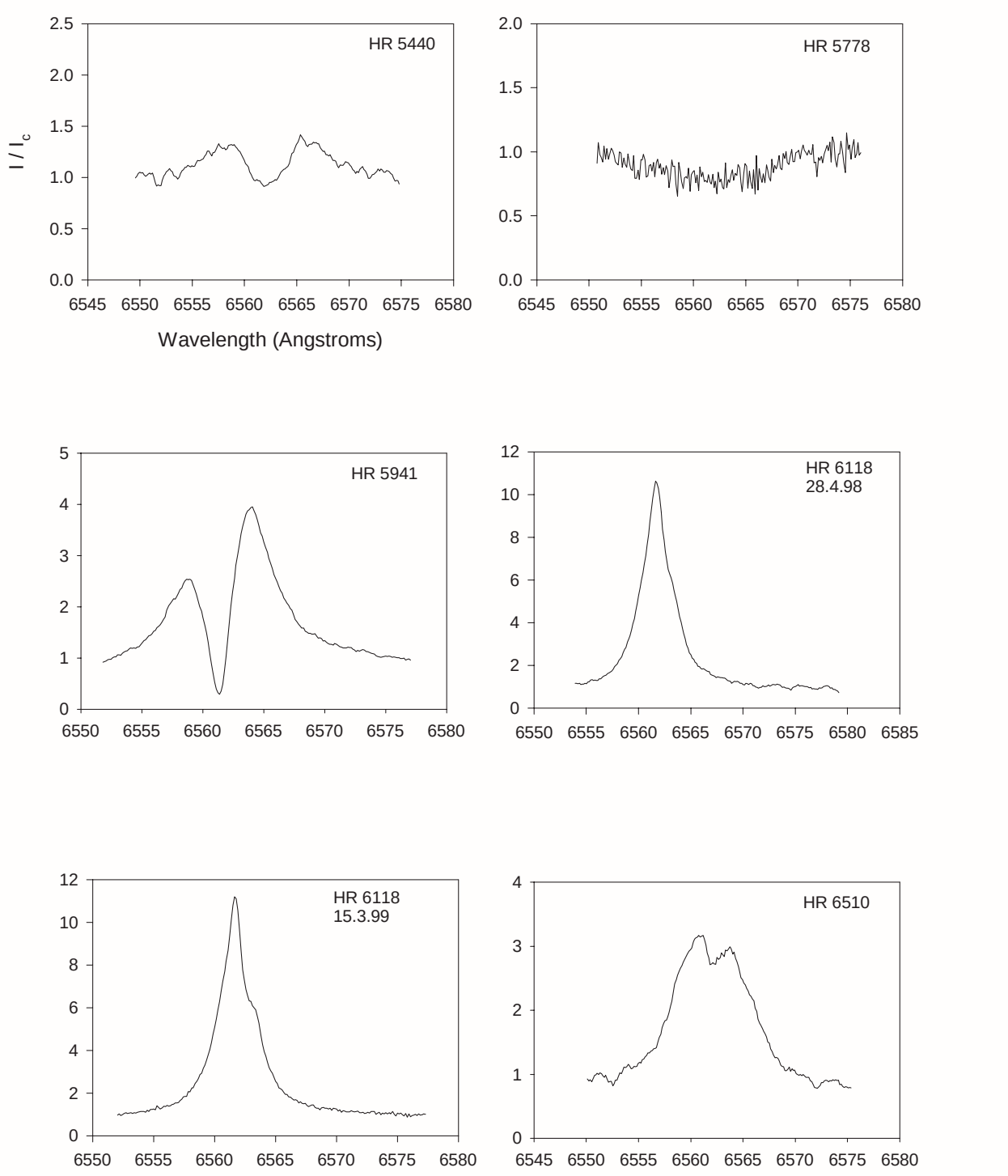

Fig. 7. Plots of the line profiles of different Be stars. The intensity plotted on the Y axis is relative and in units of the continuum level I_c

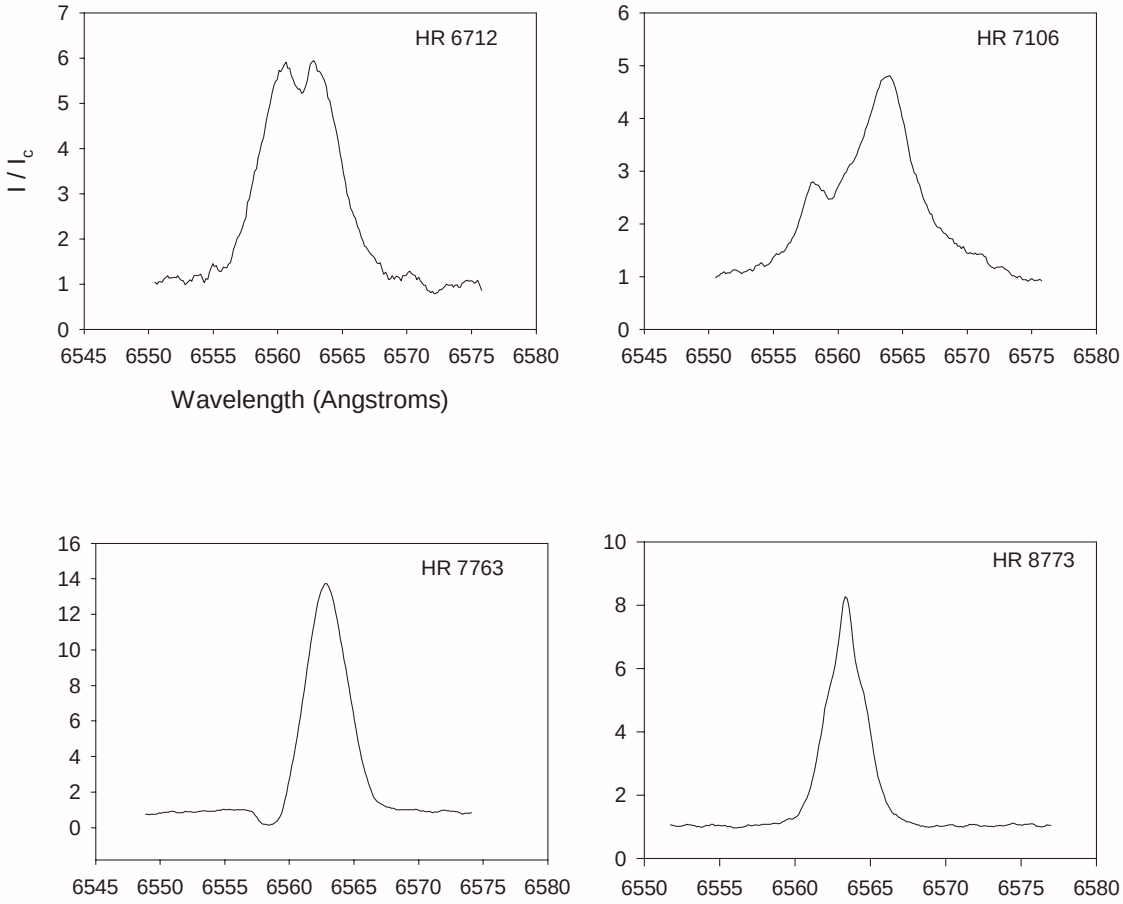

Fig. 8. Plots of the line profiles of different Be stars. The intensity plotted on the Y axis is relative and in units of the continuum level I_c

the optical fibre, is approximately 13 000 at the Hα wavelength. We have used a CCD with a Kodak KAF 1600 grade 1 chip as the detector. The main limitation of the detector is that it is only thermo–electrically cooled and does not generally permit cooling below -15 °C. Incidentally, we are trying to acquire a liquid nitrogen cooled CCD for the spectrograph with which we plan to continue the Be star programme.

All our spectra have been obtained at -15 °C. Consequently the dark count level has been just sufficient to given moderate S/N ratios in our spectra vis-a-vis those obtained by some other observers like for example Hanuschik et al. (1996). Nevertheless, our data compares reasonably well with earlier studies of Dachs et al. (1986), and Andrillat & Fehrenbach (1982), and should supplement the existing data base of emission line profiles of Be stars, especially in regards to their temporal variation. Indeed, even at its present performance level, FLAGS does provide adequate resolving power and S/N ratio to detect fine structures like wine-bottle inflections in the profiles. As pointed out by Hanuschik (1996), these structures become apparent only when high resolution and S/N profiles are available (Hanuschik 1986, 1987; Hanuschik et al. 1988; Doazan et al. 1991; Slettebak et al. 1992; Dachs et al. 1992).

The details of the observations are presented in Table 1. The table gives the HR number, the star name, the HD number, the magnitude m_v and the epoch of observation for all the stars that have been studied. Each of the spectra was obtained with an integration time of 10 min. Calibration of the wavelength scale on the detector was done using the identified lines of the solar spectrum (Kurucz et al. 1984). The rest wavelength of the laboratory Hα line was determined by using a hydrogen spectral lamp. The hydrogen lamp calibration frames were taken regularly before, in between and after the object frames to keep a check on the instrument performance and the position of the Hα rest wavelength.

3. Data reduction and analysis

Preliminary data reduction of the CCD frames, including dark subtraction and flat fielding, were done using the

Table 1.

HR No.	Name	HD No.	m_v	Epoch
193	Omi Cas	4180	4.54	23.12.98
264	Gamma Cas	5394	2.47	23.12.98
264	Gamma Cas	5394	2.47	29.11.99
335	Phi And	5394	4.25	22.12.98
496	Phi Per	10516	4.07	30.1.00
1087	Psi Per	22192	4.23	22.12.98
1165	Eta Tau	23630	2.87	30.11.99
1180	28 Tau	23862	5.09	30.11.99
1273	48 Per	25940	4.04	23.12.98
1508	56 Eri	30076	5.9	16.3.99
1622	11 Cam	32343	5.08	15.3.99
1660	105 Tau	32991	5.89	15.3.99
1789	25 Psi Ori	35439	4.95	30.1.00
1858	120 Tau	36576	5.69	14.4.99
1910	Zet Tau	37202	3	16.3.99
1934	Ome Ori	37490	4.57	22.12.98
1956	Alpha Col	37795	2.64	13.4.99
2284	FR CMa	44458	5.64	19.2.99
2343	Nu Gem	45542	4.15	12.4.99
2356	Beta MonA	45725	4.6	28.11.98
2358	Beta MonC	45727	5.6	28.11.98
2492	10 CMa	48917	5.2	23.12.98
2538	13 K Cma	50013	3.96	15.3.99
2749	28 Ome Cma	56139	3.85	20.2.99
2787		57150	4.69	14.4.99
2817		58050	6.41	26.11.98
2825		58343	5.33	20.2.99
2845	3 Beta CMi	58715	2.9	12.4.99
3135		65875	6.51	23.12.98
3237	MX Pup	68980	4.78	13.4.99
3858		83953	4.77	19.2.99
3946		86612	6.21	14.4.99
4621	Del Cen	105435	2.6	14.4.99
4696	5 Crv	107348	5.21	14.4.99
4787	5 KDra	109387	3.87	19.2.99
5193	Mu Cen	120324	3.04	21.2.99
5440	Eta Cen	127972	2.31	21.2.99
5778	4 The Crb	138749	4.14	12.4.99
5941	48 Lib	142983	4.88	15.3.99
6118	Chi Oph	148184	4.42	28.4.98
6118	Chi Oph	148184	4.42	15.3.99
6510	Alpha Ara	158427	2.95	13.4.99
6712	66 Oph	164284	4.64	12.4.99
7106	10 Beta Lyr	174638	3.45	12.4.99
7763	34 P Cyg	193237	4.81	30.11.99
8773	4 Beta Psc	217891	4.53	27.11.98

PMIS software, supplied by the CCD manufacturer. The spectra were then exported into IRAF and the physical parameters of the line profiles, such as equivalent widths, V/R ratios, half widths etc. were computed from it. A five point moving average or boxcar smoothing was done for all the spectra to reduce the noise, except in the case of HR 5778 where the spectrum was rather noisy and smoothing did not really help. The final spectra of the 44 Be stars are presented in Figs. 1–8.

Listed in Table 2 are the computed emission line parameters for the Be stars. The columns in sequential order give the HR number, the projected rotational velocity of the star $v\sin i$ in km s^{-1}, the equivalent width W in Angströms, the peak to continuum ratio $I_{\rm p}/I_{\rm c}$, the half width (i.e. full width at half maximum) l in Angströms, the full width at zero maximum E' in Angströms, the V/R ratio and the separation of the V and R components Δv in Angströms. For maintaining uniformity, we have adopted the same definitions for these terms as laid down in the paper of Andrillat (1983, refer Fig. 1), except that, following Dachs (1981), we have used a negative sign for the equivalent width when lines are in emission, and a positive sign in absorption. In some cases either the V or the R component does not form a sharp peak, but a rather extended flat/sloping region. In such cases the centre of the region has been taken for calculating the intensity of the component and measuring Δv. Such stars are marked with an asterisk in the V/R column. The majority of the m_v (Table 1) and $v\sin i$ values have been taken from an electronic version of the Bright Star Catalogue (Hoffleit & Warren 1991), but we have also referred in some cases to Dachs (1986). It may also be noted that HR 264 (Gamma Cas) and HR 6118 (Chi Oph) are repeated twice in Tables 1 and 2 since their spectra were taken at two different epochs.

We have not given the errors in the values of the above parameters for each specific star as we feel it would suffice to give only a typical range of them. The parameters which suffer most from the errors are the equivalent width W and the total width E'. In the former, the errors mainly arise when the continuum is not too well defined due to inadequate S/N. In the case of E', on the other hand, they arise when the lines are so broad that they seem to marginally extend beyond the 25 Å spectral coverage of the CCD. Using several independent measurements on IRAF, we estimate the errors in E' and W to be in the range of 5 to 10 percent. The other parameters are better defined and have errors in the range of 1 to 4 percent. As expected, smaller the S/N ratio, larger the errors.

4. Results and discussion

We find well pronounced and rather symmetric wine-bottle structures in the profiles of HR 335, 1660, 2749, 2825, 3237, 8773, and pronouncedly asymmetric wine-bottle inflexions in the profiles of HR 1622 and 6118.

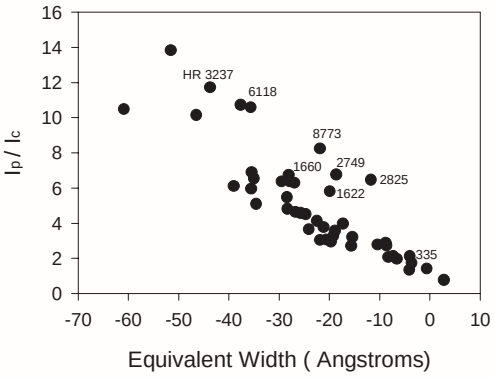

Fig. 9. A plot of the $I_{\rm p}/I_{\rm c}$ ratio versus the equivalent width, W

The average $v\sin i$ for these eight stars is 124 km s^{-1} which is well below the sample average of 236 km s^{-1}. This clearly indicates that wine-bottle structures are associated with Be stars with low inclination as shown by Hummel (1994) and Hanuschik et al. (1996). This effect can be clearly seen in Fig. 9 where we have plotted the $I_{\rm p}/I_{\rm c}$ ratio versus the equivalent width and marked the eight stars on it. From its definition, the magnitude of the equivalent width is expected to increase with an increasing $I_{\rm p}/I_{\rm c}$ ratio. This behaviour is clearly noticed in the above figure. Furthermore, however, the wine-bottle type stars plotted here, tend to lie above the general scatter, indicating that they have smaller equivalent widths (magnitude-wise) than expected from their $I_{\rm p}/I_{\rm c}$ ratio. Since the equivalent width depends on the width of the line, the reduction in the former probably indicates that the emission lines are narrower in these cases. Or, in other words, these particular stars have low $v\sin i$ values.

It may be pointed out that in twelve of the stars viz. HR 264, 496, 1087, 1789, 1858, 1910, 2356, 3858, 5440, 5778, 5941 and 7106, the line profiles appear to be broader than the 25 Å coverage of the spectrum. Therefore in Fig. 9, the equivalent widths of these stars may be marginally underestimated. However, this will not affect the above conclusions, because this underestimation, if corrected, will only enhance the separation between the wine bottle stars and the rest.

A comprehensive review of the mechanisms which broaden the line profiles has been given by Hanuschik et al. (1996). The principal amongst them are the thermal broadening, the kinematical broadening, the shear broadening (Horne & Marsh 1986) and the non-coherent scattering broadening (NSB) (Avrett & Hummer 1965; Hummel & Dachs 1992; Hummel 1994). As shown there, the amount of broadening due to each of these mechanisms depends largely on the inclination of the rotation axis of the star. For symmetrical profiles, and for most ranges of inclination (except for almost pole-on or low inclination stars), kinematic broadening is the largest and most important contributor to the profile width. The kinematic

Table 2.

HR No.	$v\sin i$ (km s^{-1})	Eq. Width W(Å)	$I_{\rm p}/I_{\rm c}$	Half Width l(Å)	Full Width E'(Å)	V/R	Δv (Å)
193	260	−29.5	6.36	5.27	13.11		
264	300	−22.47	4.12	6.07	21.33		
264	300	−26.72	4.63	6.62	23.41	1.25*	2.116
335	71	−4	2.12	3.20	6.86		
496	450	−21.88	3.03	10.69	24.63	1.01	4.11
1087	369	−39	6.11	7.40	22.28	0.98	2.86
1165	215	−8.62	2.71	5.08	12.73	1.02	1.543
1180	329	−60.93	10.48	6.03	15.31	0.92*	1.214
1273	217	−28.04	6.74	4.44	15.17		
1508	240	−24.7	4.49	6.44	20.13	0.97	1.37
1622	131	−19.92	5.80	3.69	3.94	0.72*	1.3
1660	220	−26.93	6.29	4.67	14.38		
1789	316	−15.6	2.71	9.60	17.92	1.00	5.64
1858	271	−25.73	4.57	7.83	16.12	1.02	2.29
1910	310	−20.64	3.06	9.80	22.35		
1934	194	−4.07	1.33	9.64	15.71	0.96	5.54
1956	176	−10.36	2.79	5.43	12.35	1.00	1.77
2284	265	−34.6	5.08	7.72	19.01	0.98*	1.85
2343	219	−3.64	1.73	7.76	15.86	0.86	4.07
2356	346	−24.08	3.65	9.15	19.66	1.00	3.2
2358	331	−21.1	3.78	7.30	19.28	1.32*	2.93
2492	200	−18.88	3.56	6.36	18.83	0.98	1.506
2538	199	−15.42	3.19	6.47	22.25	0.94	1.95
2749	120	−18.6	6.75	3.06	9.23		
2787	220	−28.45	5.46	5.83	12.54	1.12	2.11
2817	140	−27.88	6.38	5.12	10.81		
2825	33	−11.73	6.45	2.18	6.44		
2845	276	−6.56	1.97	6.57	13.99	1.00	2.956
3135	148	−46.53	10.13	4.19	4.41		
3237	156	−43.7	11.73	3.42	13.46		
3858	332	−19.7	2.95	9.18	20.76	1.00	2.85
3946	220	−35.03	6.53	5.65	13.66	1.02	1.355
4621	181	−35.46	6.89	5.16	17.66		
4696	−7.3	2.11	6.77	13.07	0.94	3.04	
4787	249	−8.2	2.07	7.11	16.34	1.01	2.977
5193	175	−8.75	2.89	5.12	10.28	1.03	1.77
5440	333	−0.59	1.41	13.27	22.71	0.93	7.12
5778	393	2.79	0.76	10.88	22.93		
5941	393	−17.28	3.95	7.65	22.26	0.65	5.119
6118	134	−35.63	10.58	13.09	15.86		
6118	134	−37.63	10.72	13.15	17.64	1.72*	1.4
6510	298	−19.2	3.26	8.32	18.71	1.06	2.83
6712	221	−35.53	5.97	6.97	14.88	0.99	2.07
7106	−28.36	4.80	5.80	21.95	0.58	5.802	
7763	75	−51.52	13.83	4.03	11.48	0.02	4.44
8773	128	−21.8	8.24	2.93	11.06		

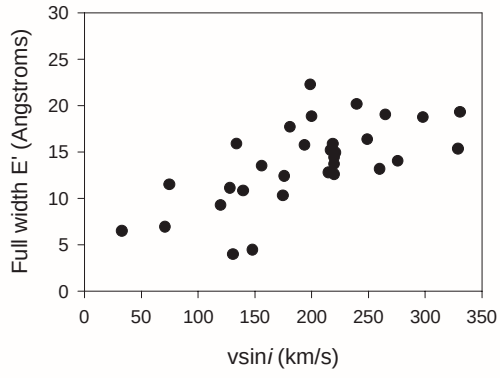

Fig. 10. A plot of the observed full widths of the lines E′ versus $v\sin i$

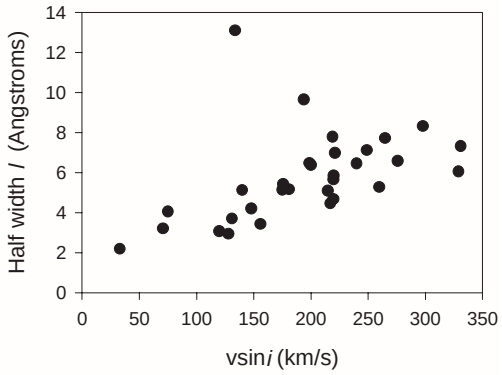

Fig. 11. A plot of the observed half widths (l) versus $v\sin i$

broadening occurs because of the supposedly Keplerian motion of the gas in the disc. Since the projected Keplerian velocity in the disc ($v_{\rm k}\sin i$) is expected to increase with the stellar rotational velocity ($v\sin i$), the observed widths of the line should also increase with the stellar $v\sin i$ values. Although simple, this scenario still gives a useful qualitative picture. In Figs. 10 and 11 we have plotted the observed fullwidths (E') and the halfwidths (l) of the profiles versus $v\sin i$. In these figures we have excluded the twelve stars mentioned in the above paragraph, which show profiles broader than 25 Å, since E' and l cannot be accurately determined for these profiles. A good correlation is seen in both the figures as found earlier too (Andrillat & Fehrenbach 1982; Dachs et al. 1986). This result tends to indicate that kinematics is the dominant factor in broadening the widths of the observed emission line profiles.

It, however, does not mean that the contribution of NSB and other mechanisms to the line widths is always negligible. NSB, in particular, is equally important in the case of low inclination or near pole-on stars as pointed out by Hanuschik (1996). In such cases, since NSB and kinematic broadening are of the same order (Hanuschik 1996), the convolution of the two is not expected to lead to a final width much different than that caused by each mechanism separately. Thus the effects of NSB

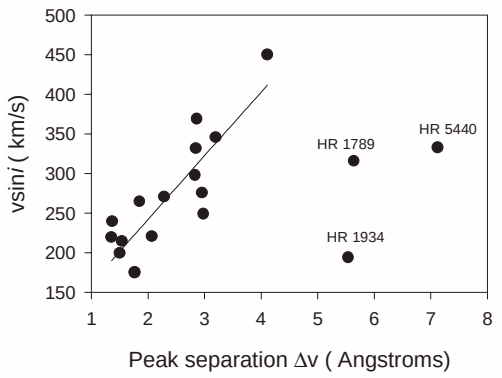

Fig. 12. A plot of $v\sin i$ versus the observed peak separation between the V and R components, Δv, for those stars that showed symmetrical profiles

broadening may be lost in the scatter of the points in Figs. 10 and 11.

Regarding the shape of the profiles, Hummel (1994) has shown how emission lines of symmetric shape, ranging from the wine-bottle structure type to the shell profiles, can be satisfactorily explained by the NSB mechanism. His model calculations show how the peak separation of the V and R components and also the equivalent width should relate to the changes in the inclination (or $v\sin i$) of the circumstellar disc. From our data we have selected nineteen sources for which the line profiles are symmetric or nearly symmetric with respect to the V and R components. These sources are HR 496, 1087, 1165, 1508, 1789, 1858, 1934, 1956, 2284, 2356, 2492, 2845, 3858, 3946, 4787, 5193, 5440, 6510 and 6712. In Fig. 12 we have plotted the peak separation Δv versus $v\sin i$. Here, barring three stars, viz. HR 1789, 1934 and 5440, the remaining stars do show Δv increasing with $v\sin i$ as expected qualitatively from the model calculations of Hummel (1994). If the above three stars are excluded, the correlation coefficient for the rest of the data comes out to be 0.72 which is rather good. A common feature in the excluded stars (HR 1789, 1934, and 5440) is that their central absorption features, on the average, are more pronounced than those of the majority of other stars of Fig. 12. It seems that for such kind of profiles the model may need some additional ingredient, but this can be verified with a larger body of data.

The equivalent width W versus Δv plot for the sample of these nineteen stars is shown in Fig. 13. Although there is only a weak correlation (correlation coefficient 0.2), a trend of W (in magnitude) decreasing with $v\sin i$ is indicated which is qualitatively consistent with the model. The scatter in Figs. 12 and 13, may be attributed to an intrinsic variation in the rotational velocities of the stars, whereas the model calculations have been made for a specific rotational velocity. In general, therefore, it is concluded that the results of Figs. 12 and 13 are consistent with the work of Hummel (1994).

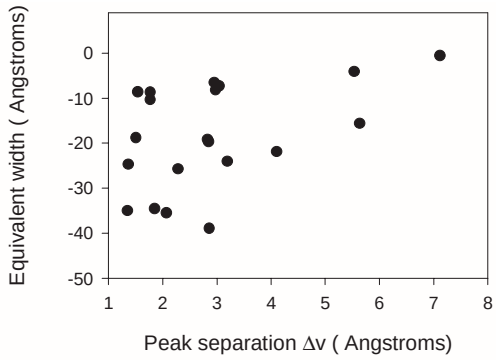

Fig. 13. A plot of the observed equivalent widths versus peak separation between the V and R components for those stars that showed symmetrical profiles

Acknowledgements. The authors wish to thank D.B. Pancholi for his able assistance on the telescope floor during some of the observational runs. We thank the referee for his valuable suggestions. The work was supported by the Department of Space, Government of India.

References

Andrillat Y., 1983, A&AS 53, 319
Andrillat Y., Fehrenbach C., 1982, A&AS 48, 93
Ashok N.M., Banerjee D.P.K., 2000, to appear in the proceedings of I.A.U Coll. 175, "The Be phenomenon in early type stars", held in Alicante, Spain (28 June - 2 July, 1999)
Avrett E.H., Hummer D.G., 1965, MNRAS 130, 295
Banerjee D.P.K., Rawat S.D., Pathan F.M., Anandarao B.G., 1999, Bull. Astr. Soc. India 27, 425
Dachs J., Eichendorf W., Schleicher H., et al., 1981, A&AS 43, 427
Dachs J., Hanuschik R.W., Kaiser D., et al., 1986, A&AS 63, 87
Dachs J., Hummel W., Hanuschik R.W., 1992, A&AS 95, 437
Doazan V., Sedmak G., Barylak M., Rusconi L., 1991, A Be star atlas, ESA SP-1147
Hanuschik R.W., 1986, A&A 166, 185
Hanuschik R.W., 1987, A&A 173, 299
Hanuschik R.W., Kozok J., Kaiser D., 1988, A&A 189, 147
Hanuschik R.W., Hummel W., Sutorius E., Dietle O., Thimm G., 1996, A&AS 116, 309
Hummel W., 1994, A&A 289, 458
Hummel W., Dachs J., 1992, A&A 262, L17
Hoffleit D., Warren W.H., 1991, The Bright Star Catalogue, revised fifth edition, Yale University Observatory
Horne K., Marsh T.R., 1986, MNRAS 218, 761
Kurucz R.L., Furenlid I., Brault J., Testerman L., 1984, Solar Atlas 1, National Solar Observatory. University Publishers, Harvard University
Slettebak A., Collins G.W., Truax R., 1992, ApJS 81, 335
Struve O., 1931, ApJ 73, 94